

# Design Considerations for Fast-Cycling Superconducting Accelerator Magnets of 2 T B-Field Generated by a Transmission Line Conductor of up to 100 kA Current

Henryk Piekarz, Steven Hays, Yuenian Huang, Vadim Kashikhin, Gijsbert de Rijk, and Lucio Rossi

**Abstract**—Recently proposed synchrotrons, SF-SPS (Super-Ferric SPS) at CERN and DSF-MR (Dual Super-Ferric Main Ring) at Fermilab, would operate with a 0.5 Hz cycle (or 2 second time period) while accelerating protons to 480 GeV. We examine possibilities of superconducting magnet technology that would allow for an accelerator quality magnetic field sweep of 2 T/s. For superconducting magnets the AC losses in the coil compromise magnetic field quality and require high level of cryogenic cooling power. We outline a novel magnet technology based on HTS superconductors that may allow reduction of AC losses in the coil possibly up to an order of magnitude as compared to similar applications with LTS type conductors.

**Index Terms**—HTS superconductor, magnet AC losses, superconducting accelerator magnets, transmission line conductor.

## I. MOTIVATION

THE long-baseline neutrino oscillation search experiments require very high intensity neutrino beams. The time-averaged power on the neutrino production target depends on the proton beam energy, proton intensity per pulse and the pulse repetition rate. As the operation of accelerators built 3–4 decades ago becomes more and more difficult they must be stopped or be replaced with new machines. This opens the opportunity to rebuild them in a way that it will suit best the needs of contemporary high-energy particle physics. For instance, with the fast cycling SF-SPS [1], in addition to improving the prospects of the neutrino physics, the LHC operations would also significantly benefit from compressed beam stacking time. The closing of the Tevatron operations in a few years will allow the use of its existing infrastructure (tunnel, cryogenic support and power distribution) for the construction of a fast-cycling dual proton synchrotron, DSF-MR [2] that would produce up to 10 MW of power at the neutrino production targets. The proposed new Fermilab layout is shown in Fig. 1. As the DSF-MR and the SF-SPS circumferences are  $\sim 6.3$  km and  $\sim 6.9$  km, respectively, a new superconducting magnet technology with

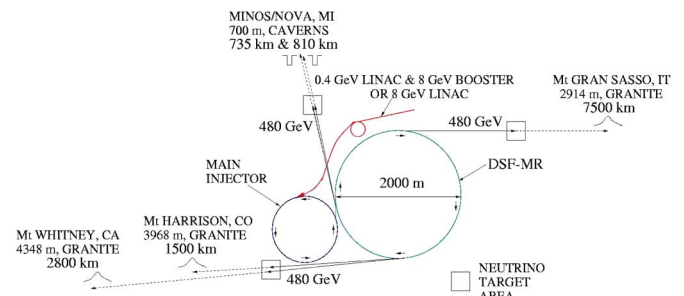


Fig. 1. The proposed accelerator complex at Fermilab with the DSF-MR accelerator. Two 480 GeV proton beams could be interchangeably extracted on up to 5 different neutrino production targets.

strongly reduced cryogenic cooling power will facilitate such undertakings.

One may observe that smaller machines, such as the Booster at Fermilab or the PS at CERN (both need to be replaced due to old age), would also greatly benefit from the new fast-cycling superconducting magnet technology. In this paper we describe magnetic and conductor designs while the matching power supply and current leads designs are presented in [3] and [4].

## II. MAGNETIC DESIGN

Assuming  $\sim 80\%$  dipole occupancy the required B-field for a 480 GeV beam in the DSF-MR and SF-SPS accelerators is  $\sim 2$  Tesla, and for 0.5 Hz cycle the dB/dt is 2 T/s. Until now all fast-cycling synchrotrons (e.g., SPS at CERN, Main Injector at Fermilab) were based on the conventional magnet technology as fast cycling superconducting magnet technology did not exist. The copper windings that powered these magnets are cooled with water while delivering the necessary current. A very serious downside of this method is the necessity of using large coils, which in turn require large cores to preserve the required high quality of the B-field in the magnet gap. However, it has been demonstrated in past few years [5], that using superconducting coils in fast-cycling magnets is more and more feasible, while reduction of the core size is typically by a factor of 10.

The window-frame magnetic core is an obvious choice due to its minimal size while allowing a high quality B-field in the magnet beam gap. For the SF-SPS and DSF-MR accelerators the magnet gap has to be no less than 40 mm. An example of the core design for such a gap using a single-turn conductor is shown in Fig. 2. In this design the weight of the core is  $\sim 230$  kg/m. This is to be compared to  $\sim 2800$  kg/m of the Fermilab Main

Manuscript received August 27, 2007. This work was supported by Fermi Research Alliance, LLC under DOE Contract DE-AC02-07CH11359.

H. Piekarz, S. Hays, Y. Huang, and V. Kashikhin are with FERMILAB, Batavia, IL 60510 USA (e-mail: hpiekarz@fnal.gov).

G. de Rijk and L. Rossi are with CERN, Geneva 23, Switzerland.

Color versions of one or more of the figures in this paper are available online at <http://ieeexplore.ieee.org>.

Digital Object Identifier 10.1109/TASC.2008.921912

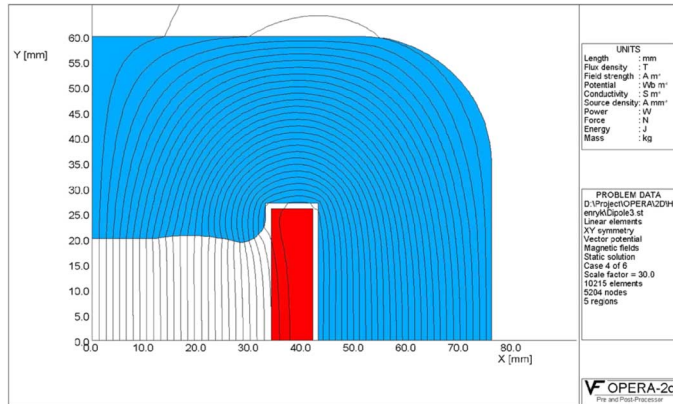


Fig. 2. B-field flux lines with a core designed for a 40 mm gap and 70 mm wide bore, 2 T fast cycling magnet powered by a transmission line conductor

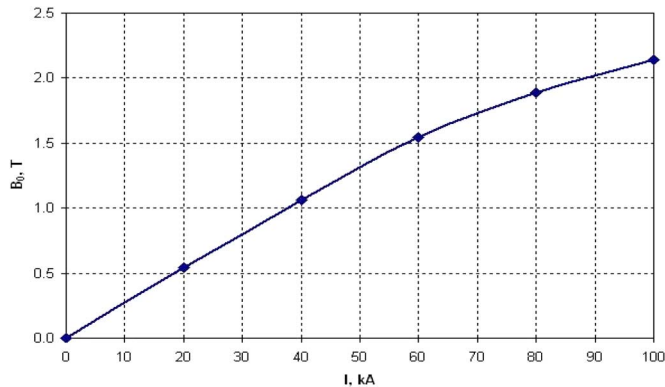


Fig. 3. The  $B(I)$  dependence for the magnetic design as shown in Fig. 2.

Injector magnet with a similar B-field and gap but based on a multiple-turn resistive conductor. The conductor cross section area in Fig. 2 is similar to superconductor design discussed in more detail in Section III.

For fast-cycling operations the magnetic cores must be made of thin, laminated soft steel plates in order to reduce the power losses induced by eddy currents. For our design we assumed that laminated, 0.1 mm thick Fe3%Si steel at room temperature was used. We project the core attributed power loss for the  $dB/dt = 2 \text{ T/s}$  and 0.5 Hz cycle to be less than 1 W/m. This is a rather small power loss that can be easily countered with a water cooling system attached to the core. One also should observe that this design produced a high uniformity in the magnetic flux along the entire width of the magnet gap.

The  $B(I)$  dependence is shown in Fig. 3. For a 2 Tesla field the required current is  $\sim 88 \text{ kA}$ . Above a current of 60 kA the response begins to deviate from linear, and the deviation reaches about 10% at 90 kA. With the AISI 1008, 1 mm thick laminated steel for the VLHC Stage 1 magnet, the deviation at 90 kA current (also 2 T field) was about 40%. With the help of correction holes in the magnet poles, however, a very high-quality magnetic field was achieved [6]. Based on this experience we expect that with some effort an even higher accelerator quality B-field can be achieved with the proposed window frame magnetic design for the fast cycling magnet.

### III. SUPERCONDUCTOR

#### A. Transmission Line Conductor Versus Coil

All past and present magnetic designs for fast-cycling accelerators are based on conductor coils comprised of multiple windings. The advantage of this approach is that it allows stacking, testing and assembling accelerator rings using single, independent magnetic elements. The disadvantage is that the multiple windings produce strong coupling between the windings leading to severe power losses. As part of the effort for the VLHC Stage 1 magnet proposal we developed a transmission line superconductor technology that is suitable for accelerator applications [7]. All magnets in the accelerator ring would be powered by a one single-turn transmission line conductor with a single set of the current leads and a common power supply. An important key to the success of transmission line conductor application is its cryogenic self-reliance, allowing for easy detachment of the conductor assembly from the magnetic core. This approach facilitates movement of the conductors to create spaces for placing corrector magnets between the magnet string cells without disconnecting the transmission-line conductors. We use our experience with the VLHC Stage 1 magnet studies and tests to make a preliminary design of a transmission line conductor for a fast cycling accelerator.

#### B. LTS Versus HTS Conductors

In the past several years there has been a great deal of effort to apply Low Temperature Superconductor (LTS) such as NbTi for fast cycling proton synchrotrons (e.g., the SIS 100 and SIS 200 accelerators at the GSI [5]). The NbTi strands are made of thousands of  $2 \mu\text{m}$ – $3 \mu\text{m}$  size filaments embedded in a Cu matrix forming a wire (strand) typically of about 0.8 mm diameter. The strands are then close packed to allow for current sharing which plays a crucial role in stabilizing of the conductor. In the AC current and AC B-field environment, however, this close packing of the strands enhances the intra-strand coupling that, combined with hysteretic losses, produces overall power losses exceeding multiple times the static losses of such conductors [5]. In addition, the problems with power losses of the LTS conductor are strongly increased due to the narrow temperature margins (1–2 K for NbTi, and 3–4 K for Nb3Sn) in which they are fully superconducting. This is regardless of the ratio of the transport current to the critical current. This very narrow temperature margin sets great demands on the efficiency and power of the cryogenic cooling system.

Until now HTS cables were not considered for fast cycling accelerator magnets in spite of a great R&D efforts aimed at their applications in generators, power transmission lines, motors and transformers with high B-field (multiple Tesla) and sweeping frequencies of up to 500 Hz. For the HTS cables LN2 at 77 K is used as a base cooling medium. In the accelerator application, however, the liquid helium coolant is the only one allowed (with exception of the LCW water) due to stringent safety requirements in the deep underground tunnels. Using the HTS conductor at 4.2 K increases multiple times its critical current. In addition, the critical current value falls typically by only about a factor of two between 4.2 K and 33 K [8] for low range, e.g., 0.5 T–1 T of the external magnetic field. With the conductor

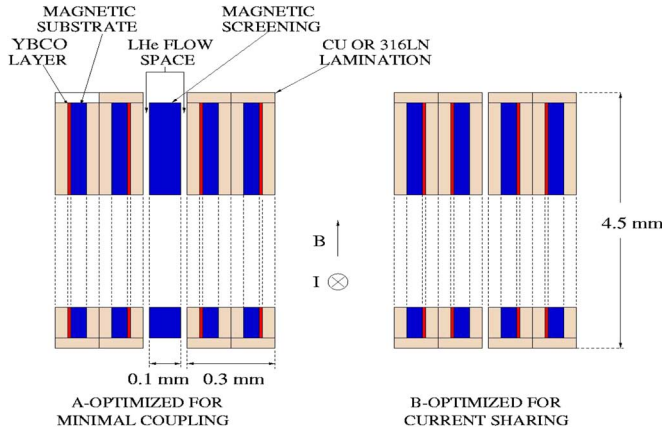


Fig. 4. Possible two arrangements of the 344/348 strands in a conductor for a dipole magnet: A—minimal coupling, and B—current sharing within a pair of strands.

line design for the transport current at  $\sim 50\%$  of the critical current, the allowable temperature margin may then be as wide as 25 K, or 10–20 times that of the LTS conductors. This feature of the HTS conductor makes it very suitable for the fast cycling operations.

#### IV. DIPOLE MAGNET WITH HTS CONDUCTOR

Contrary to the LTS wires which are typically round (or key-stone type) the HTS superconductors are predominantly produced in the form of a tape. The tape is typically  $\sim 4.5$  mm wide, and 0.15 mm–0.20 mm thick. The first generations of the HTS conductors were multi-filamentary, thus mimicking the LTS ones. The second generation HTS is based on a single filament. This approach simplified fabrication technology, lowered the cost, and most importantly produced a robust conductor that may be well suited for a large scale application. The tape can be positioned Face-On (FO) or Edge-On (EO) with respect to the sweeping magnetic field. In the FO position the critical current is reduced by as much as a factor of two, and the power losses are maximized as they are proportional to the conductor wide surface area exposed to the sweeping B-field. Contrary to that in the EO position the critical current is maximized, and the power losses are minimized as only the narrow edge of the conductor is exposed to the sweeping B-field. In the dipole magnet design with a window-frame core the magnetic flux lines cross the gap in the vertical planes parallel to the conductor wide surface. This represents an ideal case for using the HTS superconductor tapes in the EO formation. In Fig. 4, two possible arrangements of two pairs of the 2G-344/348 tapes of the American Superconductor [9] are shown. These superconductor tapes which are 4.5 mm wide and (0.15–0.20) mm thick primarily consist of a thin,  $2 \mu\text{m}$  YBCO layer,  $50 \mu\text{m}$ – $75 \mu\text{m}$  Ni-Alloy substrate, and 316LN or Cu  $\sim 50 \mu\text{m}$  thick lamination covering the assembly of the superconductor strand. As the  $\mu_{\text{rel}}$  for the Fe3%Si steel in the core is  $\sim 2500$  the magnetic flux can be mostly pulled out of the conductor area as indicated in Fig. 2. In this core design, effort was focused on extending as much as possible the good field region through the entire width of the magnet gap. As a result some 25% of the flux (or  $\sim 0.5$  T) is passing through the conductor. For a fast cycling magnet one should naturally focus on

TABLE I  
POWER LOSS IN 344/348 TAPES

Strand component	Case I [mW/m]	Case II [mW/m]
YBCO, $2 \mu\text{m}$	0.050	0.380
Hustelloy underlayer, $50 \mu\text{m}$	$< 0.0001$	0.005
Overlayer, Ag, $3 \mu\text{m}$	$< 0.0001$	$< 0.0001$
Ni5%W sub. + scr., $100 \mu\text{m}$	0.136	0.136
AC current/self-field, $i = 0.5$	0.088	0.088
AC current/AC field, $i = 0.5$	$< 0.0001$	0.002
Cu lamination, 0.1 mm	0.0095	0.038
316LN lamination, 0.1 mm	0.0167	0.067
Total with Cu lamination	0.284	0.649
Total with 316LN lamination	0.291	0.678

minimizing the flux in the conductor area though it will be at expense of some reduction in the usable width of the magnet gap.

There is an interesting situation, however, with the 2G 344/348 superconductors. They use a slightly magnetic substrate to support the YBCO layer. This helps to confine self-fields into the area closest to the conductors. It was demonstrated in [10] that by arranging two tapes with back-to-back substrates (as in Fig. 4) self-fields of the neighboring YBCO conductors cancel (as the currents flow in the same direction self-fields circulate in the opposite directions in the area between the conductors), and so these two conductors become de-coupled. In order to de-couple the “pairs” in a multi-strand conductor assembly we added an additional Ni-Alloy tape between them as shown in the left side of Fig. 4, though studies [11] with NbTi cored Rutherford cable showed strong coupling suppression just with thin SS foils. On the right side of Fig. 4 the YBCO strips are facing each other so that the copper lamination allows for current sharing between them thus increasing stability, but the coupling losses are cut only by half. Each type of the strand arrangements in the Fig. 4 should significantly suppress not only the coupling losses but also the hysteretic losses as the multiple magnetic substrates minimize the flux crossing the superconductor strip. The  $\mu_{\text{rel}}$  of Ni-Alloy substrate used in the 2G-344/348 tapes is not known but it could be as high as 200, or  $\sim 8\%$  of that of the magnetic core. So, the external flux in the conductor area has to be reduced to  $< 160$  mT for these Ni-Alloy substrates and foils to be very effective.

Scaling from a very thorough power loss analysis of YBCO conductor in [12] we evaluate the power losses for the 2G-344/348 tapes. The results are summarized in Table I. We consider 2 cases: I—ideal one with all magnetic flux parallel to superconductor strip, and II—with 50% of the magnetic flux crossing conductor at  $\sim 50^\circ$  angle, as indicated in Fig. 2. The YBCO conductor losses are hysteretic ones, the over-layer and under-layer are eddy current type. The Ni5%W layer losses are of eddy current type but they depend only on the frequency as the B-field saturates in them. The Cu and 316LN steel losses are of the eddy current type. The AC current and AC field losses are evaluated for a transport current at  $\sim 50\%$  of the critical one. As the coupling losses saturate to the hysteretic losses one must add 1/2 YBCO hysteretic losses for the B type arrangement in Fig. 4, but cut by  $\sim 1/3$  the Ni5%W substrate loss (no screen there). For further discussion we choose the current sharing

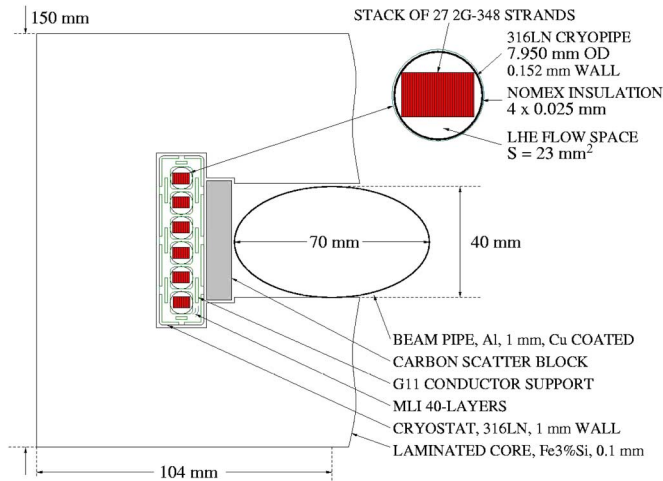


Fig. 5. Arrangement of magnetic core, HTS conductor and beam pipe for the DSF-MR/SF-SPS main arc dipole magnet.

option which also means using a Cu lamination instead of steel. The total projected loss is 0.284 mW/m for the Case I, and 0.649 mW/m for the Case II.

### V. DSF-MR/SF-SPS MAIN ARC DIPOLE MAGNET

A possible arrangement of the DSF-MR/SF-SPS main arc magnet is illustrated in Fig. 5. As the static losses give a rather significant contribution, we use our experience with the VLHC transmission line design to outline the one with HTS strands. There will be a total of 162 conductor strands arranged in 6 subsets, each with 27 strands. With 162 strands at 4.5 K the 88 kA transport current is about 1/2 of the critical current [8]. Each conductor subset is placed inside a 316LN pipe (8 mm OD, 0.152 mm wall) rated for 40 bar allowable, 200 bar ultimate pressure. The helium flow space for 6 pipes is  $\sim 150 \text{ mm}^2$  with helium contact area to the strands of  $\sim 80\%$ . Each pipe is insulated with 4 layers of 0.025 mm Nomex tape providing  $\sim 3 \text{ kV}$  breakdown protection. The pipe assemblies are supported by G11 rings inside the 316LN cryostat with a 1 mm wall. This cryostat is a squared pipe but the core walls and a carbon block provide additional strong support. Some 40 layers of MLI are wrapped around the 6 pipe assemblies. The projected static heat load is  $\sim 0.18 \text{ W/m}$  per conductor, or  $0.36 \text{ W/m}$  of magnet, being about 2 1/2 times higher than the  $0.14 \text{ W/m}$  expected static loss for the VLHC Stage 1 magnet [7].

The total power losses for a 1 m long magnet are listed in Table II. For a comparison we also show the projected losses for a Nuclotron dipole [5] based on the NbTi conductor, all for 0.5 Hz and  $\text{dB}/\text{dt} = 2 \text{ T/s}$ . Although there is some uncertainty about the proposed application of the HTS conductor due to small amount of ferromagnetic material embedded in it Table II shows that there is a potential for a strong reduction of the cryogenic power demand, perhaps up to an order of magnitude with respect to NbTi conductor. This, if true, will make fast-cycling large superconducting accelerators well acceptable.

The vertical orientation of the HTS tapes in the conductor assembly facilitates their bending in the horizontal plane. This

TABLE II  
MAGNET POWER LOSS WITH HTS AND NbTi STRANDS

Magnet type	Coil [W/m]	Static [W/m]	Total W/m	Accelerator 7000 m, [kW]
Case I	0.092	0.360	0.452	3
Case II	0.210	0.360	0.570	4
Nuclotron	3	2	5	35

helps bypassing the corrector magnet set at half cell, and to counter the cryogenic shrinkage of a long transmission line.

### VI. SUMMARY AND CONCLUSIONS

We made a very preliminary study of application feasibility of the HTS superconductor for fast cycling transmission-line, super-ferric accelerator magnets. It seems that there exists a potential for minimization of the power losses associated with fast cycling accelerators. The initiation of an R&D program for fast cycling accelerator magnets powered by HTS type superconductors is well warranted.

### ACKNOWLEDGMENT

The authors are greatly indebted to Cees Thieme of the AMSC for several illuminating conversations.

### REFERENCES

- [1] G. Ambrosio, S. Hays, Y. Huang, J. Johnstone, V. V. Kashikhin, J. MacLachlan, N. Mokhov, H. Piekarz, T. Sen, V. Shiltsev, G. de Rijk, and L. Rossi, "LER-LHC injector workshop summary and super-ferric fast cycling injector in the SPS tunnel," in *CARE-HHH-APD, LHC LUMI-06*, Valencia, 2006.
- [2] H. Piekarz and S. Hays, "Preliminary consideration of a dual, 480 GeV, fast cycling accelerator for production of neutrino beams at Fermilab," in *TM-2381-AD-TD*, 2007.
- [3] S. Hays, H. Piekarz, H. Pfeffer, and B. Claypool, "Design consideration of a power supply system for fast cycling superconducting accelerator magnets operating at 2 tesla and 100 kA," in *MT-20*, 2007.
- [4] Y. Huang, S. Hays, H. Piekarz, G. de Rijk, and L. Rossi, "Design considerations of a pair of power leads for fast cycling accelerator magnets operating at 2 tesla and 100 kA," in *MT-20*, 2007.
- [5] G. Moritz, "Superconducting magnets for the 'International Accelerator Facility for Beams of Ions and Antiprotons' at GSI," *IEEE Trans. Appl. Supercond.*, vol. 13, no. 2, pp. 1329–1334, 2003.
- [6] G. Velev, W. Foster, V. Kashikhin, P. Mazur, A. Oleck, H. Piekarz, P. Schlabach, C. Sylvester, and M. Wake, "Field quality measurements of a 2 tesla transmission line magnet," *IEEE Trans. Appl. Supercond.*, vol. 16, no. 2, pp. 1840–1843, 2006.
- [7] G. Ambrosio *et al.*, "Design study for a staged very large hadron collider," in *Fermilab-TM-2149*, 2001.
- [8] D. Turrioni, E. Barzi, M. Lamm, V. Lombardo, C. Thieme, and A. V. Zlobin, "Angular measurements of HTS critical current for high field solenoids," in *CEC/JCMC*, 2007, submitted for publication.
- [9] A. P. Malozemoff, 2nd Gen. HTS Wire [Online]. Available: www.am-super.com 2004
- [10] O. Tsukamoto, A. K. M. Alamgir, M. Liu, D. Miyagi, and K. Ohmatsu, "AC loss characteristics of stacked conductors composed of HTS coated conductors with magnetic substrates," *IEEE Trans. Appl. Supercond.*, vol. 17, pp. 3195–3198, 2007.
- [11] M. N. Wilson *et al.*, "Cored Rutherford cables for the GSI fast ramping synchrotron," *IEEE Trans. Appl. Supercond.*, vol. 13, no. 2, pp. 151–156, 2003.
- [12] M. D. Sumption, E. W. Collings, and P. N. Barnes, "AC loss in stripped YBCO conductors leading to designs for high frequencies and field-sweep amplitudes," *Superconductor Science & Technology*, vol. 18, p. 122, 2005.